Phase imaging for absorptive phase objects using hybrid uniform and structured illumination Transport of Intensity Equation

Yunhui Zhu,[1*] **Zhengyun Zhang,**[2] **and George Barbastathis**[1,2]

[1]*Department of Mechanical Engineering, Massachusetts Institute of Technology, 77 Massachusetts Avenue, Cambridge, Massachusetts, 02139, USA*
[2]*Singapore-MIT Alliance for Research and Technology (SMART) Centre, 1 Create Way, 138602, Singapore*
**yunhui@mit.edu*

Abstract: Transport of intensity equation (TIE) has been a popular and convenient phase imaging method that retrieves phase profile from the measurement of intensity differentials. Conventional 2-shot uniform illumination TIE can give reliable inversion of the phase from intensity in many situations of practical interest; however, it has a null space consisting of fields with non–zero circulation of the Poynting vector. Here, we propose the hybrid illumination TIE method to disambiguate such objects. By comparing the diffraction signals using uniform and structured (sinusoidal) illumination patterns, we obtain a modulation-induced signal that depends solely on the phase gradient. In this way, we also increase signal sensitivity in the low spatial frequency region.

OCIS codes: (100.5070) Phase retrieval; (110.4280) Noise in imaging systems; (110.2945) Illumination design; (100.3010) Image reconstruction techniques.

References and links

1. F. Zernike, "Phase contrast, a new method for the microscopic observation of transparent objects," Physica **9**, 686–698 (1942).
2. K. A. Nugent, D. Paganin, and T. E. Gureyev, "A phase odyssey," Phys. Today **54**, 27–32 (2001).
3. P. B. Bach, J. R. Jett, U. Pastorino, M. S. Tockman, S. J. Swensen, and C. B. Begg, "Computed tomography screening and lung cancer outcomes," Jama **297**, 953–961 (2007).
4. GERCHBER. RW, and W. Saxton, "Phase determination from image and diffraction plane pictures in electron-microscope," Optik **34**, 275 (1971).
5. J. R. Fienup, "Reconstruction of an object from the modulus of its fourier transform," Opt. Lett. **3**, 27–29 (1978).
6. M. Reed Teague, "Deterministic phase retrieval: a green's function solution," J. Opt. Soc. Am. A **73**, 1434–1441 (1983).
7. W. Hoppe, "Trace structure analysis, ptychography, phase tomography," Ultramicroscopy **10**, 187–198 (1982).
8. T. Gureyev, A. Roberts, and K. Nugent, "Partially coherent fields, the transport-of-intensity equation, and phase uniqueness," J. Opt. Soc. Am. A **12**, 1942–1946 (1995).
9. D. Paganin and K. A. Nugent, "Noninterferometric phase imaging with partially coherent light," Phys. Rev. Lett. **80**, 2586 (1998).
10. T. Gureyev, Y. I. Nesterets, D. Paganin, A. Pogany, and S. Wilkins, "Linear algorithms for phase retrieval in the fresnel region. 2. partially coherent illumination," Opt. Commun. **259**, 569–580 (2006).
11. R. Lewis, "Medical phase contrast x-ray imaging: current status and future prospects," Phys. Med. Biol. **49**, 3573 (2004).

#225559 - $15.00 USD Received 27 Oct 2014; revised 31 Oct 2014; accepted 2 Nov 2014; published 12 Nov 2014

12. L. Waller, S. S. Kou, C. J. Sheppard, and G. Barbastathis, "Phase from chromatic aberrations," Opt. Express **18**, 22817–22825 (2010).
13. L. Allen and M. Oxley, "Phase retrieval from series of images obtained by defocus variation," Opt. Commun. **199**, 65–75 (2001).
14. L. Waller, L. Tian, and G. Barbastathis, "Transport of intensity phase-amplitude imaging with higher order intensity derivatives," Opt. Express **18**, 12552–12561 (2010).
15. L. Waller, M. Tsang, S. Ponda, S. Y. Yang, and G. Barbastathis, "Phase and amplitude imaging from noisy images by kalman filtering," Opt. Express **19**, 2805–2814 (2011).
16. J. A. Schmalz, T. E. Gureyev, D. M. Paganin, and K. M. Pavlov, "Phase retrieval using radiation and matter-wave fields: Validity of teague's method for solution of the transport-of-intensity equation," Phys. Rev. A **84**, 023808 (2011).
17. A. Lubk, G. Guzzinati, F. Börrnert, and J. Verbeeck, "Transport of intensity phase retrieval of arbitrary wave fields including vortices," Phys. Rev. Lett. **111**, 173902 (2013).
18. A. Shanker, L. Tian, M. Sczyrba, B. Connolly, A. Neureuther, and L. Waller, "Transport of intensity phase imaging in the presence of curl effects induced by strongly absorbing photomasks," Appl. Opt. **53**, J1–J6 (2014).
19. A. Shanker, M. Sczyrba, B. Connolly, F. Kalk, A. Neureuther, and L. Waller, "Critical assessment of the transport of intensity equation as a phase recovery technique in optical lithography," in "SPIE Advanced Lithography," (International Society for Optics and Photonics, 2014), pp. 90521D–90521D.
20. A. Shanker, L. Tian, and L. Waller, "Defocus-based quantitative phase imaging by coded illumination," in "SPIE BiOS," (International Society for Optics and Photonics, 2014), pp. 89490R–89490R.
21. Y. Zhu, A. Pan, and G. Barbastathis, "Low-noise tie phase imaging by structured illumination," in "Computational Optical Sensing and Imaging," (Optical Society of America, 2014), pp. CTh3C–5.
22. Y. Zhu, A. Shanker, L. Tian, L. Waller, and G. Barbastathis, "Low-noise phase imaging by hybrid uniform and structured illumination transport of intensity equation," Opt. Express **22**, 26696–26711 (2014).
23. M. R. Dennis, K. O'Holleran, and M. J. Padgett, "Singular optics: optical vortices and polarization singularities," Progress in Optics **53**, 293–363 (2009).
24. L. Allen, H. Faulkner, K. Nugent, M. Oxley, and D. Paganin, "Phase retrieval from images in the presence of first-order vortices," Phys. Rev. E **63**, 037602 (2001).
25. D. Paganin, A. Barty, P. McMahon, and K. Nugent, "Quantitative phase-amplitude microscopy. iii. the effects of noise," J Microsc. **214**, 51–61 (2004).
26. L. Turner, B. Dhal, J. Hayes, A. Mancuso, K. Nugent, D. Paterson, R. Scholten, C. Tran, and A. Peele, "X-ray phase imaging: Demonstration of extended conditions for homogeneous objects," Opt. Express **12**, 2960–2965 (2004).
27. L. Tian, J. C. Petruccelli, and G. Barbastathis, "Nonlinear diffusion regularization for transport of intensity phase imaging," Opt. Lett. **37**, 4131–4133 (2012).
28. K. Ichikawa, A. W. Lohmann, and M. Takeda, "Phase retrieval based on the irradiance transport equation and the fourier transform method: experiments," Appl. Opt. **27**, 3433–3436 (1988).
29. F. Pfeiffer, T. Weitkamp, O. Bunk, and C. David, "Phase retrieval and differential phase-contrast imaging with low-brilliance x-ray sources," Nat. Physics **2**, 258–261 (2006).
30. P. Pérez, M. Gangnet, and A. Blake, "Poisson image editing," in "ACM Transactions on Graphics (TOG)," , vol. 22 (ACM, 2003), vol. 22, pp. 313–318.
31. M. R. Hestenes and E. Stiefel, *Methods of Conjugate Gradients for Solving Linear Systems*, (National Bureau of Standards, 1952, vol. 49).

1. Introduction

Conventional imaging cameras, in both the visible and x–ray regimes, can only record the time-averaged intensity of the light field. However, it has been known for a long time [1] that the phase of the electromagnetic field has a stronger signature from the optical path length (OPL) of objects that light has gone through and therefore provides much richer information about semitransparent objects of interest. Phase retrieval has recently become a vibrant research topic due to advances in optical technology, especially digital cameras, opto–mechanics, and computing. Advances of phase imaging are summarized in an excellent survey [2]. Representative examples with great practical significance are biological cells in the visible range and low–Z materials in the x–ray range [3].

To record the phase delay quantitatively with conventional intensity cameras, it is required that phase information be mapped onto the intensity distribution. Until the early 1970's, it used to be thought that the only physical way to produce this mapping of phase onto inten-

#225559 - $15.00 USD Received 27 Oct 2014; revised 31 Oct 2014; accepted 2 Nov 2014; published 12 Nov 2014

sity is interferometry. However, the seminal papers by Gerchberg-Saxton [4] and Fienup [5] challenged this assumption for the first time. Follow–up challenges came in the early 1980's with propagation–based methods, such as Teague and Stroebl's transport of intensity (TIE) method [6] and Hoppe's ptychography [7]. These techniques have become nowadays extremely popular: avoiding interferometry offers significant advantages, for example reduced need for mechanical stability, easier application to the non–visible regime, especially x–rays, and partially coherent fields [8–11].

In this paper, we are interested in the Transport of intensity Equation (TIE), which in principle obtains the phase information from the measurement of the intensity differential upon propagation over a short distance downstream the optical axis. There are alternatives, for example extraction of the OPL from color dispersion in a defocused imaging system [12] and schemes exploiting multiple (more than two) measurements downstream to improve robustness of the differential measurement to noise [13–15]

The intensity differential signal, which is used to retrieve the phase, turns out to equal the divergence of the Poynting vector [9]. However, this divergence signal is independent of the circulation component of the Poynting vector. In other words, the circulation (curl) component of the Poynting vector is "invisible" in the TIE measurement. As a result, previous TIE phase imaging has been limited necessarily to situations where the Poynting vector is curl-free [6,8,9]. Otherwise, the TIE phase retrieval method will generate intrinsic errors or even fail.

Strong absorption gradients usually generate the circulation effect [16], therefore in applications of the TIE strongly absorptive objects have been generally avoided. There are a couple of special absorptive situations where the original TIE method is still valid (see next section), or it can become valid using a modified TIE solver with additional boundary conditions [17]. Iterative methods have also been proposed to partially correct for the error introduced by the circulation effect from strong absorption [18]. However, a large range of interesting partially absorbing objects still cannot be properly handled by the TIE method due to the circulation effect, examples including bone boundaries in bio x-ray images, and edge effect from lithography photomasks [19].

As a better alternative, here we present hybrid structured illumination to solve the TIE circulation problem for imaging phase objects with general absorption profiles. Our method works by using a known structured illumination to convert the curl component into visible divergence terms. By comparing the diffraction intensity patterns with and without structured illumination, we are able to separate the modulation induced diffraction signal that is directly dependent on the phase gradient rather than the divergence of the Poynting vector. As a result, we are able to retrieve the phase profile accurately despite the presence of strong circulation effect.

In addition, as argued in previous works [20–22], the hybrid structured illumination TIE greatly enhances the robustness of the retrieved absorption and phase to noise. This is because the high–frequency features of the structured illumination enhance light diffraction thus combating the tendency of TIE to perform poorly at low spatial frequencies. In the case of general absorptive objects that we consider in the present paper, there is an additional important benefit: in the hybrid structured illumination case, the differential signal used to recover the phase is obtained from a fixed location but with two different illumination patterns. An in–focus signal is still required for normalization, but the end result is much less sensitive to errors in the amount of defocus, misalignment, etc.

The rest of this paper is organized as follows. We discuss circulation effect in the conventional uniform illuminated TIE in Sec. 2. The theoretical treatment of hybrid structured illumination TIE is presented in Sec. 3. Simulation and experimental implementation of this method is demonstrated in Sec. 4, where the hybrid illumination phase retrieval results are compared to the conventional TIE phase retrievals. Conclusions and discussions are presented in Sec. 5.

#225559 - $15.00 USD Received 27 Oct 2014; revised 31 Oct 2014; accepted 2 Nov 2014; published 12 Nov 2014

2. Uniform illuminated TIE and circulation effect

Consider the propagation of the intensity profile I. Suppose a thin target object with phase $\phi(x,y)$ and transmission $T(x,y)$ is located at $z=0$. Let $I(x,y;d)$ denote the intensity after propagation by a (small) distance d behind the object or its conjugate in a suitable imaging system. When explicit reference to the lateral coordinates can be omitted without risk of confusion, we will abbreviate as $I(d)$. The TIE equation demonstrated that the intensity differential $\partial I(x,y;z)/\partial z$ along the propagation axis z induced by Fresnel propagation is relate to the phase profile $\phi(x,y)$ and intensity profile $I(x,y;0)$ by

$$k\frac{\partial I(x,y;z)}{\partial z}\bigg|_{z=0} = -\nabla_\perp \cdot \Big(I(x,y;0)\nabla_\perp \phi(x,y)\Big), \tag{1}$$

where x and y are coordinates in the plane perpendicular to the propagation z axis, k is the wave number of the optical field, and $\nabla_\perp \equiv (\mathbf{i}\partial/\partial x + \mathbf{j}\partial/\partial y)$, is the gradient operator on the $x-y$ plane, with $\mathbf{i}$ and $\mathbf{j}$ being the unit direction vector in the x and y directions, respectively. For a semi-monochromatic light field with central frequency ω, the Poynting vector S is expressed by the intensity I and phase ϕ profiles as [9]

$$\vec{S} = \frac{\omega}{4\pi} I\nabla\phi. \tag{2}$$

We recognize that the TIE intensity differential is the divergence of the Poynting vector in the $x-y$ plane.

Conventional TIE phase imaging uses uniform incident illumination. The technique is well known and we repeat here for comparison and to establish notation. Denote the intensity of the uniform illumination by U_0. The intensity distribution right after the thin object is $I(0)=U_0T$. Inserting it into Eq. (1) yields

$$-\frac{1}{k}\nabla_\perp \cdot (U_0T\nabla_\perp\phi) = \frac{\partial I}{\partial z} \simeq \frac{I(d)-U_0T}{d} \equiv \frac{\Delta(d)}{d}, \tag{3}$$

where $\Delta(d)$ is the intensity differential signal. Conventionally, a 2-shot measurement of intensity images both in focus and defocused by d is used to obtain the intensity differential $\Delta(d)$ and the transmission profile T, as shown in Fig. 2(a).

For a general absorptive phase object under uniform illumination U_0, the Poynting vector may contain both circulation and divergence components. In other words, $T\nabla_\perp\phi$ can be decomposed by

$$T\nabla_\perp\phi = \nabla_\perp \times C(x,y) + \nabla_\perp D(x,y), \tag{4}$$

where $\nabla_\perp \times \equiv (-\mathbf{i}\partial/\partial y + \mathbf{j}\partial/\partial x)$ is the curl operator on the $x-y$ plane, $\nabla_\perp \times C(x,y)$ and $\nabla_\perp D(x,y)$ are the circulation and the divergence terms, respectively. Inserting Eq. (4) into Eq. (3), the circulation component $\nabla_\perp \times C(x,y)$ disappears and the TIE equation reduces to a Poisson's Equation

$$\nabla_\perp^2 D(x,y) = -\frac{k}{dU_0}\Delta(d), \tag{5}$$

which can be solved to resolve the divergence part of $T\nabla_\perp\phi$. The circulation component, on the other hand, is lost in the TIE measurement and cannot be retrieved.

The solution of $D(x,y)$ is useful in the phase retrieval only when the Poynting vector is curl free. In such cases, the phase is retrieved by the well-known solver [9]

$$\phi_u(x,y) = -k\nabla_\perp^{-2}\left\{\nabla_\perp \cdot \left[\frac{1}{T}\nabla_\perp D(x,y)\right]\right\}, \tag{6}$$

#225559 - $15.00 USD Received 27 Oct 2014; revised 31 Oct 2014; accepted 2 Nov 2014; published 12 Nov 2014

where ϕ_u refers to the phase reconstruction with uniform illumination. The non-circulation condition requires that

$$\nabla_\perp \times (T\nabla_\perp \phi) = \nabla_\perp T \times \nabla_\perp \phi = 0. \tag{7}$$

Equation (7) is satisfied in the following three situations [6, 8–10, 19].

- $\nabla_\perp T = 0$. This is true for a transparent (pure phase) object with uniform illumination. In this case, the intensity profile I is constant and there is no intensity gradient, so the TIE holds without ambiguity.
- $\nabla_\perp T(x,y) = 0$ while $\nabla_\perp \phi(x,y) \neq 0$. In this case, the intensity profile is locally uniform in locations where the phase has spatial variations. One common example is a piecewise constant phase object with a small absorber, e.g. a. piece of dust. Such intensity variations will not introduce a circulation effect.
- $\nabla_\perp T \parallel \nabla_\perp \phi$. This happens when the object satisfies a phase-attenuation duality condition, *i.e.* at frequencies away from resonance. Then, the phase ϕ becomes proportional to the absorbance $-\ln(T)$ of the object. With uniform illumination, the gradient vectors of the phase and the intensity are parallel to each other. As a result, the cross product is zero.

In general, the cross product of the gradients can be non-zero since the transmission and OPL of the object are not necessarily correlated, especially at optical frequencies that, for most materials, are far from resonance. For example, the circulation effect may occur for overlapped objects with different phase/absorbance proportionalities, for objects that disobey the phase-attenuation duality, or when there is a gradient in the illumination itself—though in this paper we actually show how to use a special gradient to our advantage against this problem.

As an example of how Poynting vector circulation can be generated in a relatively simple configuration, in Fig. 1 we show the overlapped two partially absorbing spheres of different materials. When there is overlap, misalignment of the phase gradient and the intensity gradient (as shown in Fig. 1(c)) produces a circulation component in the Poynting vector under uniform illumination. Inserting the calculated intensity differential $\Delta(d)$ from Eq. (3) into Eq. (6), a phase reconstruction is obtained and shown in Fig. 1(d). We see that Eq. (6) generates artifacts in the overlapped region as a result of circulation effect.

It is also noted that Poynting vector circulation can also be induced by one or more phase vortices [2]. In such cases, circulation Poynting vector with zero divergence is introduced by phase singularity points [23]. One well-known case is the hypergeometric-Gaussian beam with a spiral phase profile. An intensity-null point in the center displays a phase singularity. Such phase profiles are also "invisible" in conventional uniform illumination TIE method. Vortex components have been shown to be recovered using multiple intensity measurements along the propagating axis [24]. It is also trackable using the hybrid illumination TIE method, introducing in the next section.

3. Hybrid illumination TIE phase imaging with absorptive phase object and the correction of the circulation effect

In this section, we introduce the hybrid illumination TIE phase imaging method to correct for the circulation-induced errors. The hybrid illumination TIE imaging setup is conceptually shown in Fig. 2(b). We use structured illumination with an intensity profile denoted by $U_s(x,y)$. The intensity profile right after the target object becomes $U_s(x,y)T(x,y)$. Inserting it into the TIE Eq. (1) yields

$$-\frac{1}{k}\nabla_\perp \cdot (U_s\, T\, \nabla_\perp \phi) = \frac{\partial I}{\partial z} \simeq \frac{I_s(d) - U_s\, T}{d}, \tag{8}$$

#225559 - $15.00 USD Received 27 Oct 2014; revised 31 Oct 2014; accepted 2 Nov 2014; published 12 Nov 2014

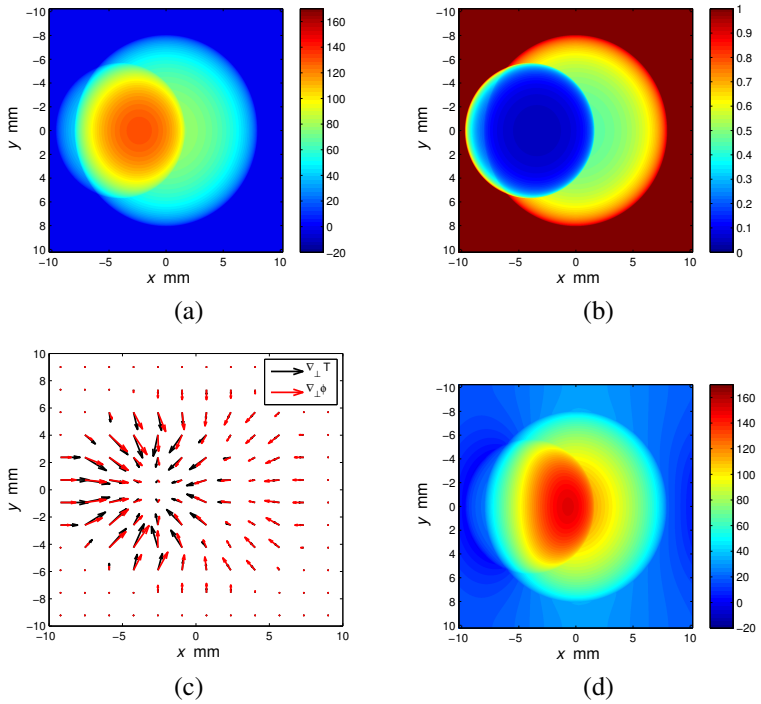

Fig. 1. Aberration in uniform illumination TIE phase retrieval with a 2-ball object. The absorbance of the smaller ball is twice as strong as the bigger ball, while the refractive index of the smaller ball is half as much as that of the bigger ball. Figure (a) and (b) show the phase profile ϕ (in rad) and the transmission T respectively. Figure (c) shows the gradient vectors of the transmission and phase. Misalignment is seen in the overlapping areas. Figure (d) shows the phase retrieval result ϕ_u using Eq. (6). Aberration is observed in the overlapping area where circulation effect occurs.

where $I_s(x,y;d)$ denotes the transverse intensity profile at distance d with the structured illumination U_s. Now consider the absorptive phase object with a circulation effect under uniform illumination. Inserting Eq. (4) into Eq. (8), we obtain

$$-\frac{1}{k}\left[\nabla_\perp U_s \cdot \Big(\nabla_\perp \times C(x,y) + \nabla_\perp D(x,y)\Big) + U_s \nabla_\perp^2 D(x,y)\right] = \frac{I_s(d) - U_s\, T}{d}. \tag{9}$$

We see that the previously invisible circulation component now contributes to the diffraction signal through the interaction with the structured illumination. Furthermore, a structure induced diffraction signal $s(d)$ is extracted by combining Eqs. (3) and (8) such that

$$\begin{aligned} -\frac{1}{k}\left[\nabla_\perp \cdot (U_s\, T\, \nabla_\perp \phi) - U_s \nabla_\perp \cdot (T\, \nabla_\perp \phi)\right] = \\ = \frac{I_s(d) - U_s\, T - U_s/U_0\, \Delta(d)}{d} = \frac{I_s(d) - U_s/U_0\, I(d)}{d}, \end{aligned} \tag{10}$$

which is simplified as

$$\nabla_\perp U_s \cdot \nabla_\perp \phi = -\frac{k}{dT}\left(I_s(d) - \frac{U_s}{U_0} I(d)\right) \equiv -\frac{k}{d} s(d). \tag{11}$$

#225559 - $15.00 USD Received 27 Oct 2014; revised 31 Oct 2014; accepted 2 Nov 2014; published 12 Nov 2014

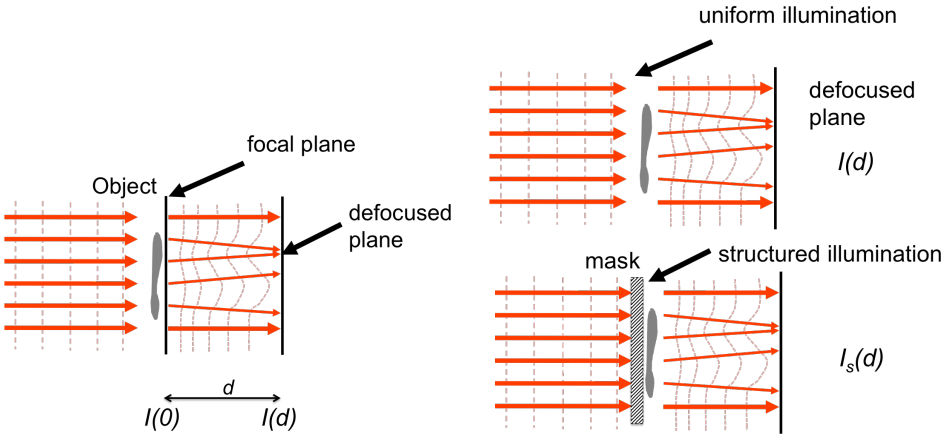

(a) conventional 2-shot TIE (b) hybrid illuminationTIE

Fig. 2. Conceptual setup of the conventional 2-shot TIE (a) and the hybrid illumination TIE (b). Intensity differentials are obtained via displacement of CCD and via changing the illumination pattern, respectively.

Here, $s(d)$ is determined solely by the illumination structure and phase gradients; the dependence is immune to circulation effect. Also note that the differential signal is obtained by comparing the intensities $I_s(d)$ and $I(d)$ at the same defocused location d, whereas the in–focus measurement $I(0) = T\,U_0$ is only used for normalization. Compared to the conventional 2–shot TIE, which extracts phase information by comparing the intensity profiles at two different locations $I(d)$ and $I(0)$ (shown in Fig. 2(a)), the hybrid illumination TIE is much less sensitive to misalignment errors. In experiments with short defocused distances, the in–focus measurement can be conveniently approximated with the low–pass filtered version of $I(d)$, allowing for 2-shot imaging operation without any displacement of the camera.

In addition, the new phase imaging method also increases the signal sensitivity. According to Eq. (3), the intensity differential signal $\Delta(d)$ results from taking the gradient on the phase profile twice. As a result, the differential signal is highly sensitive to the high spatial frequency features of the phase profile, but is not very responsive to low frequency components. The low sensitivity in the low frequency region leads to the low frequency noise corruption problem for TIE phase retrieval [14, 25]. Although the low frequency noise can be removed via the linear Tikhonov regularizer [26] or a nonlinear method utilizing the sparsity priors [27], regularizer performance is limited by the condition of the forward problem; here, high frequency features in the structured illumination essentially improve the condition of the forward problem in TIE.

Equation (11) can be inverted to obtain the phase gradient along the gradient direction of the structured illumination U_s. Although the optical phase profile ϕ can be determined from the phase differential in one direction alone, it is generally beneficial to obtain phase differentials in both orthogonal directions for noise suppression [22]. In the simplest case that we investigate here, we use sets of orthogonal and shifted sinusoidal structured illumination patterns as

$$\begin{aligned} U_{s,X}(x,y) &= aU_0\left(1+\eta\sin(2\pi f_m x)\right), \\ U_{s,Y}(x,y) &= aU_0\left(1+\eta\sin(2\pi f_m y)\right); \end{aligned} \tag{12}$$

#225559 - $15.00 USD Received 27 Oct 2014; revised 31 Oct 2014; accepted 2 Nov 2014; published 12 Nov 2014

$$
\begin{aligned}
U_{q,X}(x,y) &= aU_0\left(1+\eta\cos(2\pi f_m x)\right),\\
U_{q,Y}(x,y) &= aU_0\left(1+\eta\cos(2\pi f_m y)\right),
\end{aligned}
\tag{13}
$$

where a is the intensity gain/attenuation, η is the modulation depth, and f_m is a suitably selected spatial frequency, and the subscript q stands for "quadrature". As explained in [22], the quadrature (shifted by 90°) patterns are needed to eliminate "blind spots" due to the zero gradient at the peaks and troughs of the original pattern Eq. (12). Following the same procedure as in [22], we obtain the inverse estimates

$$
\begin{aligned}
\phi_x &= -\frac{k}{d}\frac{1}{aU_0\eta\ 2\pi f_m}\left(s_X(d)-is_{q,X}(d)\right)e^{-i2\pi f_m x}\\
\phi_y &= -\frac{k}{d}\frac{1}{aU_0\eta\ 2\pi f_m}\left(s_Y(d)-is_{q,Y}(d)\right)e^{-i2\pi f_m y}.
\end{aligned}
\tag{14}
$$

Up to here the acquisition method requires a total of six intensity images: uniform illumination in and out of focus, two orthogonal patterns, and two quadrature patterns. To reduce the number of measurements to four, a simplification can be made for smooth objects. When the spectrum of the phase differential is negligible beyond the modulation frequency f_m, the quadrature measurements in Eq. (13) can be omitted. In this case, the shifted spectrum lobes in the positive and negative regions are are no longer overlapping and can thereby be separated. Intuitively speaking, the bandwidth constraint means that there are no fine features to be imaged in–between the fringes of the illumination pattern. Consequently, the "blind spot" is not a problem anymore. Without the quadrature, the simpler estimate of the phase gradients is obtained in the frequency domain as

$$
\begin{aligned}
\phi_x &= \mathscr{F}^{-1}\left[i\frac{k}{d}\frac{1}{\pi f_m a\eta U_0}\mathscr{F}\left(s_X(d)\right)(u+f_m,v)\cdot H_x(u,v)\right]\\
\phi_y &= \mathscr{F}^{-1}\left[i\frac{k}{d}\frac{1}{\pi f_m a\eta U_0}\mathscr{F}\left(s_Y(d)\right)(u,v+f_m)\cdot H_y(u,v)\right],
\end{aligned}
\tag{15}
$$

where $\mathscr{F}$ is the Fourier transform operator, u,v are the spatial frequency coordinates in the Fourier domain, $H_x(u,v)=\exp(-u^2/f_m^2)$ and $H_y(u,v)=\exp(-v^2/f_m^2)$ are the low-pass filters in the x and y directions, respectively. Note that the lateral shear interferometer [28] can be considered as a special case of hybrid TIE for extremely smooth objects whose own diffraction can be ignored. Also note that the structured illumination TIE is different from grid-based Talbot interferometry [29] in that the propagation distance d is far smaller than the Talbot distance, which allows for more compact imaging systems, especially in the x-ray region.

The phase gradient's profiles obtained either from Eq. (15) for low-pass objects or Eq. (14) for high-frequency signals can be used as the final result in cases where the phase differential is of interest. Alternatively, the phase profile ϕ can be obtained according to various reconstruction techniques, including direct integration or regularized direct inversion using the Fourier transform [22]. The former may yield inconsistent results depending on integration path, and the latter assumes periodic boundary conditions and requires regularization to remove the singularity at zero frequency. In this paper, we create an estimate ϕ_h of the phase by minimizing the squared error between the gradient of the estimate and the measured gradient, effectively solving a discretized Poisson equation with boundary conditions [30]. We use conjugate gradients [31] to minimize this positive semi-definite quadratic function with regularized Fourier-based inversion as a preconditioner to speed up convergence. This approach allows us to handle arbitrary phase boundaries while still minimizing the error with respect to the measurements. Although the regularization in the preconditioner affects convergence rate, it does not directly impact the residual.

#225559 - $15.00 USD Received 27 Oct 2014; revised 31 Oct 2014; accepted 2 Nov 2014; published 12 Nov 2014

4. Simulation and experimental implementation of the hybrid illumination TIE phase imaging

We implement the hybrid structured illumination TIE phase imaging method through both simulation and experiment. We compare the phase retrieval results with the uniform TIE phase imaging results. The comparison shows that and the hybrid illumination method not only corrects for the circulation-effect induced aberration but also substantially increases the sensitivity.

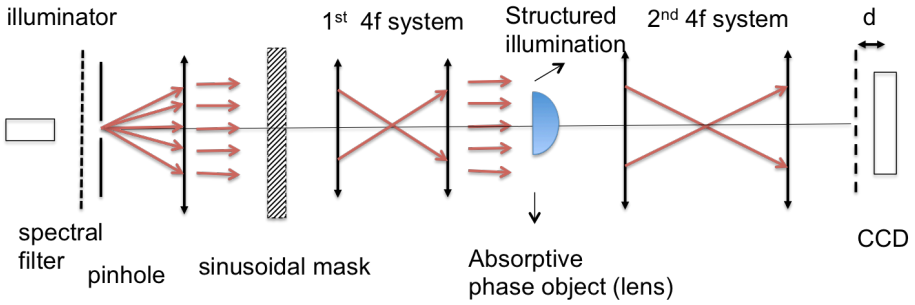

Fig. 3. Experiment setup of the hybrid structured illumination TIE.

We build a TIE phase imaging system as Fig. 3. A broadband LED fiber illuminator is used as the light source. A narrowband filter (bandwidth 1 nm, central wavelength 633 nm) and a pinhole (diameter 50 μm) are used to increase the temporal and spatial coherence of the illumination light field. The filtered light cone is converted into parallel beams via a lens. A sinusoidal absorptive mask is placed at the left side of the first 4-f system; the fringes are imaged onto the image plane on the right side of the 4-f system as the structured illumination. An absorptive phase object is placed on the imaging plane of the first 4-f system. A second 4-f system then images the absorptive phase object onto a CCD detector. The CCD is placed near the focal plane of the second 4-f system. By moving the CCD along the optical axis, we make intensity measurements both in-focus and defocused by d. The pixel size of the CCD is 4.4 μm. We obtain the phase images using both the 2-shot uniform and the hybrid illumination TIE method. For the uniform illumination 2-shot TIE phase imaging, we take one in-focus image and one defocused image with uniform illumination. For the hybrid structured illumination TIE phase imaging, we take two additional defocused images with sinusoidal structured illumination aligned in the x and y directions, respectively.

We uses a calibrated half-ball lens as the phase object. The lens is immersed in index-matching oil, and the effective phase profile is calibrated in Fig. 4(b). A gradient absorption filter is placed close to the lens to provide some arbitrary absorption profile $T(x,y)$ with a strong intensity gradient. The absorption profile is captured by the in-focus intensity measurement shown in Fig. 5(a) and simulated in Fig. 4(a).

We first simulate the phase imaging using a Fresnel propagation kernel. The uniform illumination TIE phase retrieval result ϕ_u, obtained by Eq. (6), is shown in Fig. 4 (c). In this result, the intensity profile obtained by the CCD is assumed to be noiseless. However, we still observed phase aberration as if the lens has been compressed in the vertical y direction. This is expected since the gradient of the absorption is mainly aligned horizontally. As a result, phase reconstruction is affected in places where the phase gradient has a vertical component. Fig. 4(d) shows the

#225559 - $15.00 USD Received 27 Oct 2014; revised 31 Oct 2014; accepted 2 Nov 2014; published 12 Nov 2014

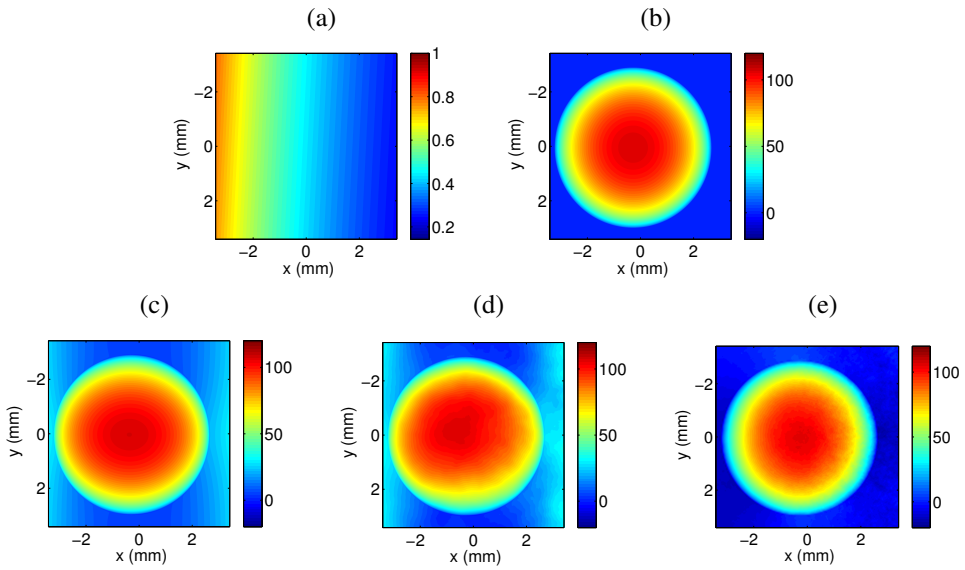

Fig. 4. Simulated TIE phase imaging results of a half-spherical lens with gradient absorption background. (a), in-focus intensity profile $I(0)$ (normalized); (b), calibrated phase profile ϕ; (c) uniform illumination TIE phase retrieval without noise $\phi_u^{\text{noiseless}}$; (d) uniform illumination TIE phase retrieval with noise ϕ_u^{noisy} and (e) hybrid illumination TIE phase retrieval with noise ϕ_h^{noisy}. (d) and (e) both use a noise power of -25 dB in the intensity simulation. Other parameters used in the simulation include the modulation attenuation $a = 0.5$, modulation depth $\eta = 0.4$ and the modulation frequency $f_m = 0.0103\ \mu\text{m}^{-1}$.

uniform illumination TIE phase retrieval results with noise. In this simulation, a noise with a normalized intensity power of -25 dB is applied to the measured intensity profile. As a result of the low responsibility in the low frequency region, the phase retrieval is severely contaminated by low-frequency noise. Fig. 4(e) shows the result ϕ_h^{noisy} using the hybrid illumination TIE method. A same noise power of -25 dB is applied to the simulation. We see that aberration is corrected and noise is largely reduced demonstrating the advantage of the hybrid illumination method.

We next measure the phase profile using the experiment setup shown in Fig. 3. The results shown in Fig. 5 agree to the simulation very well. We first obtain the phase retrieval results using uniform illumination TIE. A low-noise version is obtained by using 10 times as much as exposure time in each intensity measurement. Figure 5(c) shows the low-noise result. We see aberration in the vertical direction, as expected. Next, we restore the normal exposure time and obtain a noisy result shown in Fig. 5(d). The phase retrieval is severally contaminated by low-frequency noise and aberration. In contrast, by applying the same normal exposure time in the hybrid illumination TIE phase imaging, we obtain an aberration-free symmetric phase retrieval result, as shown in Fig. 5(e). Compared to Fig. 5(d), the aberration induced by the circulation effect has been corrected, and the noise has been suppressed, showing a significantly enhanced sensitivity of the signal. On the down side, the boundary of the sphere is smeared in the hybrid illumination TIE result ϕ_h. This is caused by the low frequency filter used in Eq. (15). High frequency features beyond f_m can be reserved using the quadrature method.

#225559 - $15.00 USD Received 27 Oct 2014; revised 31 Oct 2014; accepted 2 Nov 2014; published 12 Nov 2014

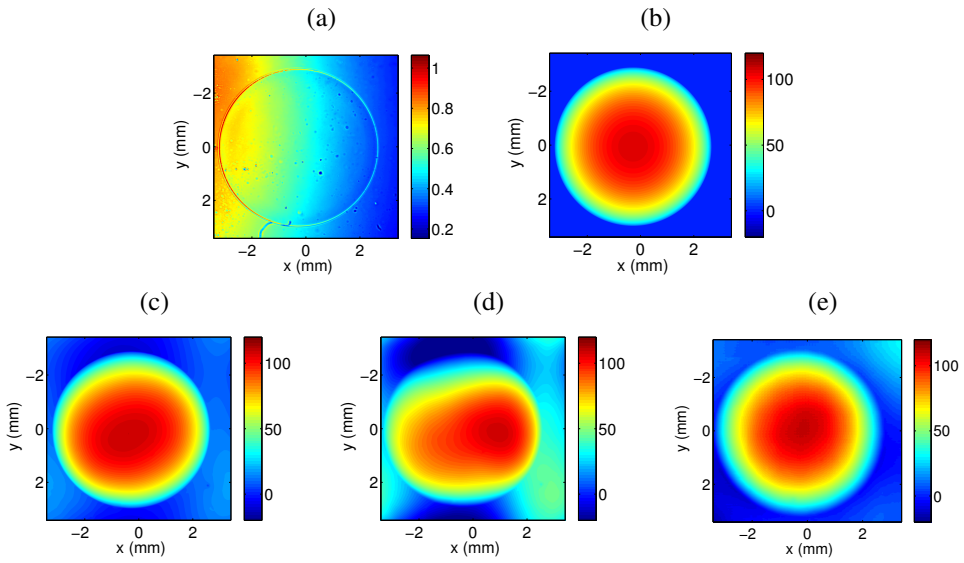

Fig. 5. Experimental TIE phase imaging results of a half-spherical lens with gradient absorption background. (a), experimental measurement of in-focus (normalized) intensity profile $I(0)$; (b) expected phase profile ϕ; (c), highly exposed ($10\times$ exposure time) uniform illumination TIE phase retrieval $\phi_u^{\text{less noisy}}$, (d) normally exposed ($1\times$ exposure time) uniform illumination TIE phase retrieval ϕ_u^{noisy}, and (e) hybrid illumination TIE phase retrieval ϕ_h^{noisy} ($1\times$ exposure time). In the experiment, the modulation attenuation $a = 0.31$, modulation depth $\eta = 0.4$ and the modulation frequency $f_m = 0.0103\ \mu\text{m}^{-1}$.

5. Conclusion

We have demonstrated both theoretically and experimentally that an accurate and robust phase retrieval is obtained using the hybrid illumination TIE method. The method enables propagation based TIE phase imaging to general phase/absorption objects that have been previously considered only possible with interferometric methods. Future work will focus on case-specified optimization of the illumination pattern, application of this method to the imaging of phase vortices, and utilizing sparsity or other compressive priors to enhance the quality of the phase imaging.

Acknowledgments

This research was funded by the US Department of Homeland Security. We would like to acknowledge Laura Waller and Lei Tian for helpful discussions.

#225559 - $15.00 USD Received 27 Oct 2014; revised 31 Oct 2014; accepted 2 Nov 2014; published 12 Nov 2014